T-matrix calculations for the electron-impact ionization of hydrogen in the Temkin-Poet model

M. S. Pindzola, D. Mitnik, and F. Robicheaux

Department of Physics, Auburn University, Auburn, Alabama 36849

An eigenchannel *R*-matrix expansion of the *T* matrix is used to calculate total integrated and ejected energy differential cross sections for the electron-impact ionization of hydrogen in the Temkin-Poet model. In previous close-coupling results, unphysical oscillations in the total ionization cross section could be averaged over due to the smooth dependence of the cross section on the incident energy. For differential ionization cross sections, a step-function behavior in the cross sections' overall ejected energy dependence has made unphysical oscillation removal much more problematic. By formulation design, the *T*-matrix method eliminates the step-function problem found in most close-coupling calculations of the ejected energy differential cross section. Total and differential ionization cross sections in a one-state *R*-matrix expansion are in excellent agreement with Hartree-Fock distorted-wave results. Total and differential ionization cross sections in multiple state *R*-matrix expansions converge toward the more accurate results given by a time-dependent wave-packet method. Unphysical oscillations appear in the differential ionization cross sections for all the *T*-matrix results involving more than three states in the *R*-matrix expansion, but the oscillations are small, symmetric about $E/2$, and easily averaged to give a smooth uniform result.

I. INTRODUCTION

Over the last few years several nonperturbative methods have been developed to treat the quantal three-body problem found in the direct electron-impact ionization of atoms and ions. All of the methods were first tested on the Temkin-Poet [1,2] model for hydrogen, beginning with a direct numerical integration of the time-independent Schrödinger equation and a close-coupling calculation with pseudostates by Callaway and Oza [3]. In subsequent years the two-dimensional *R*-matrix [4], converged close-coupling [5], hyperspherical close-coupling [6], eigenchannel *R*-matrix [7], time-dependent wave-packet [8], *R*-matrix with pseudostates [9], and exterior complex scaling [10] methods have all produced total ionization cross sections in excellent agreement with those of Callaway and Oza [3].

On the other hand, an accurate calculation of the ejected energy differential cross section for singlet scattering in the Temkin-Poet model has proved to be a more difficult theoretical challenge [11–14]. In the close-coupling methods unphysical oscillations appear in both the total integrated and ejected energy differential cross sections. The oscillations are due in part to a finite basis set description of the continuum and the imposition of two-body boundary conditions for a three-body problem. For the total ionization cross sections the unphysical oscillations can be averaged over due to the underlying smooth dependence of the cross section on the incident energy [5,7,9]. For the differential ionization cross sections, a step-function behavior in the cross section's overall ejected energy dependence has made unphysical oscillation removal much more difficult [9,11–14].

In this paper we calculate total and energy differential cross sections for electron-impact ionization of hydrogen in the Temkin-Poet model using a method based on an eigenchannel *R*-matrix expansion of the *T* matrix and compare those results with those from a time-dependent wave-packet method. All first-order perturbation theory methods using

distorted-waves begin with a zeroth-order approximation for the scattered wave function in the exact *T* matrix [15]. In a natural extension, an *R*-matrix expansion of the scattered wave function may be used to include higher-order perturbative effects in the *T* matrix. The same procedure has proved quite successful in calculating accurate dipole matrix elements for the photoionization of atoms, beginning with the pioneering work of Burke and Taylor [16]. A compelling reason for investigating the *T*-matrix method is that it formally eliminates the step-function problem [9,11–14] found in many close-coupling calculations of the ejected energy differential cross section. The wave-packet method has been used previously to examine the threshold law for total ionization cross sections in various *s*-wave models [17]. Its extension to energy differential cross sections [18,19] is based on the asymptotic relationship between the two-electron coordinate and momentum spaces [20]. Since the time-dependent wave-packet method is free of oscillations, it is used here as a standard to compare against the *T*-matrix method. The time-dependent wave-packet and time-independent *R*-matrix methods are presented in Sec. II, total and energy differential cross sections for the electron-impact ionization of hydrogen in the Temkin-Poet model are presented in Sec. III, and a brief summary is found in Sec. IV. Atomic units are used throughout the paper, unless specifically indicated.

II. THEORY

A. Time-dependent wave-packet method

The time-dependent wave-packet expression for the direct ionization of hydrogen in the Temkin-Poet model for singlet scattering is given by [17,19]

$$\sigma = \frac{\pi}{4k_i^2} \int_0^E \frac{d\epsilon_e}{k_e k_f} \mathcal{P}(k_i, k_e, k_f), \tag{1}$$

where the linear momenta (k_i, k_e, k_f) correspond to the incoming, ejected, and outgoing electron, respectively. The total energy $E = \epsilon_i + I = \epsilon_e + \epsilon_f$, where $\epsilon = k^2/2$ and $I = \frac{1}{2}$ is the ionization energy of hydrogen. The scattering probability is given by

$$
\begin{aligned}
&\mathcal{P}(k_i, k_e, k_f) \\
&= \left| \int_0^\infty dr_1 \int_0^\infty dr_2 \bar{P}_{k_e}(r_1) \bar{P}_{k_f}(r_2) P(r_1, r_2, t=T) \right|^2.
\end{aligned}
\tag{2}
$$

The two-dimensional wave function $P(r_1, r_2, t)$ is a solution to the time-dependent Schrödinger equation given by

$$
i \frac{\partial P(r_1, r_2, t)}{\partial t} = H(r_1, r_2) P(r_1, r_2, t),
\tag{3}
$$

where

$$
H(r_1, r_2) = -\frac{1}{2} \frac{\partial^2}{\partial r_1^2} - \frac{1}{2} \frac{\partial^2}{\partial r_2^2} - \frac{1}{r_1} - \frac{1}{r_2} + \frac{1}{\max(r_1, r_2)}.
\tag{4}
$$

The initial condition for the solution of the time-dependent Schrödinger equation is given by

$$
P(r_1, r_2, t=0) = \sqrt{\frac{1}{2}} [\bar{P}_{1s}(r_1) G_{k_i}(r_2) + G_{k_i}(r_1) \bar{P}_{1s}(r_2)],
\tag{5}
$$

where $G_k(r)$ is a radial wave packet. The wave function at a time $t = T$ following the collision is obtained by propagating Schrödinger's equation on a two-dimensional spatial lattice. The bound $\bar{P}_{ns}(r)$ and continuum $\bar{P}_k(r)$ orbitals needed in the above equations are obtained by diagonalization of the single-particle Hamiltonian

$$
h(r) = -\frac{1}{2} \frac{\partial^2}{\partial r^2} - \frac{1}{r}
\tag{6}
$$

on a one-dimensional spatial lattice.

B. Time-independent T-matrix method

The time-independent T-matrix expression for the direct ionization of hydrogen in the Temkin-Poet model for singlet scattering is given by [15]

$$
\sigma = \frac{8}{k_i^2} \int_0^E \frac{d\epsilon_e}{k_e k_f} |T(k_i, k_e, k_f)|^2,
\tag{7}
$$

where the transition matrix is

$$
T(k_i, k_e, k_f) = \int_0^\infty dr_1 \int_0^\infty dr_2 P_{k_e}^C(r_1) P_{k_f}^C(r_2)
$$

$$
\times \frac{1}{\max(r_1, r_2)} P_E^+(r_1, r_2),
\tag{8}
$$

and $P_k^C(r)$ are Coulomb continuum orbitals with normalization chosen as 1 times a sine function.

1. Distorted-wave method

A zeroth-order approximation for the outgoing two-dimensional wave function $P_E^+(r_1, r_2)$ is given by

$$
P_E^+(r_1, r_2) = \sqrt{\frac{1}{2}} [P_{1s}(r_1) P_{k_i}^{HF}(r_2) + P_{k_i}^{HF}(r_1) P_{1s}(r_2)].
\tag{9}
$$

The bound orbitals $P_{ns}(r)$ are hydrogenic, while the distorted-wave orbitals $P_k^{HF}(r)$ are solutions of the Hartree-Fock equation

$$
\left(h(r) + V_D + V_X - \frac{k^2}{2} \right) P_k^{HF}(r) = 0,
\tag{10}
$$

where the direct potential operator is given by

$$
V_D P_k^{HF}(r) = \int_0^\infty \frac{P_{1s}^2(r')}{\max(r, r')} dr' P_k^{HF}(r),
\tag{11}
$$

and the exchange potential operator by

$$
V_X P_k^{HF}(r) = \int_0^\infty \frac{P_{1s}(r') P_k^{HF}(r')}{\max(r, r')} dr' P_{1s}(r)
$$

$$
+ \left(\epsilon_{1s} - \frac{k^2}{2} \right) \int_0^\infty P_{1s}(r') P_k^{HF}(r') dr' P_{1s}(r).
\tag{12}
$$

The continuum normalization for the Hartree-Fock distorted waves is chosen as $\sqrt{1/k}$ times a sine function. We note that the full nonlocal exchange term found in Eq. (12), including the exchange-overlap term, is needed to make accurate calculations for the T matrix and ionization cross sections.

2. R-matrix method

In principle, a more accurate approximation for the outgoing two-dimensional wave function $P_E^+(r_1, r_2)$ is

$$
P_E^+(r_1, r_2) = \sum_k \alpha_{Ek}^J P_k(r_1, r_2),
\tag{13}
$$

where R-matrix theory is used to obtain the complex expansion coefficients α_{Ek}^J for the confined box states $P_k(r_1, r_2)$. The two-dimensional eigenstates $P_k(r_1, r_2)$ and eigenenergies E_k are obtained by diagonalization of the two-particle Hamiltonian

$$\mathcal{H}(r_1,r_2)=H(r_1,r_2)+\frac{1}{2}\delta(r_1-R)\frac{\partial}{\partial r_1}$$

$$+\frac{1}{2}\delta(r_2-R)\frac{\partial}{\partial r_2}, \qquad (14)$$

using a basis of symmetrized products of single-particle orbitals,

$$\bar{P}_k(r_1,r_2)=\mathcal{S}\sum_n\sum_{n'}\bar{P}_n(r_1)\bar{P}_{n'}(r_2), \qquad (15)$$

where $\mathcal{S}$ is a symmetrization operator and the single-particle bound and continuum orbitals $\bar{P}_n(r)$ are themselves obtained by diagonalization of the $h(r)$ of Eq. (6) on a one-dimensional lattice with boundary conditions of either $\bar{P}(r=R)=0$ or $\partial\bar{P}(r=R)/\partial r=0$. The Bloch operators of Eq. (14) ensure that the matrix representation of $\mathcal{H}(r_1,r_2)$ is Hermitian. The wave-function expansion is characterized by the number of states n for the "bound" electron and the number of states n' for the "continuum" electron found in Eq. (15). The number of states in an R-matrix expansion refers to n, while n' is assumed to be large enough to represent the scattered electron. The lowest-energy states in the R-matrix expansion are generally bound and spectroscopic, while the higher-energy states may be in the continuum and are generally labeled as "pseudostates." The eigenchannel R-matrix method [7], which we use here, makes use of many single particle orbitals with boundary condition $\bar{P}(r=R)=0$ and only one with boundary condition $\partial\bar{P}(r=R)/\partial r=0$.

For outgoing wave boundary conditions, the complex expansion coefficients are given by [16]

$$\alpha_{Ek}^{J}=\frac{1}{2(E_k-E)}\sum_n w_{nk}(R)\frac{\partial F_{n1}^{J}(R)}{\partial r}, \qquad (16)$$

where the surface amplitudes $w_{nk}(R)$ define the standard R matrix:

$$R_{nn'}=\frac{1}{2R}\sum_k\frac{w_{nk}(R)w_{n'k}(R)}{E_k-E}. \qquad (17)$$

For scattering from the ground state, $n'=1$, the boundary derivatives of the outgoing wave asymptotic solutions $F_{nn'}^{J}(r)$ for all open channels n are given by

$$\frac{\partial F_{n1}^{J}(R)}{\partial r}=\sqrt{k_n}\sum_{n''}^{open}(\delta_{nn''}\cos k_n R-K_{nn''}\sin k_n R)J_{n''1}, \qquad (18)$$

while for all closed channels n they are given by

$$\frac{\partial F_{n1}^{J}(R)}{\partial r}=-\kappa_n\sum_{n''}^{open}K_{nn''}e^{-\kappa_n R}J_{n''1}. \qquad (19)$$

The K matrix is related to the R matrix in the standard manner, while the J matrix is defined by:

$$J_{nn'}=(1-iK)_{nn'}^{-1}. \qquad (20)$$

A one-state R-matrix calculation for $P_E^+(r_1,r_2)$, involving the ground state orbital, is equivalent to the zeroth-order distorted-wave solution of Eq. (9). As one includes more states in the R-matrix calculation for $P_E^+(r_1,r_2)$, the calculation for the T matrix, and the direct ionization cross section, should become more accurate.

We note that, since we have already determined the K matrix in the above procedure, we may easily determine the S matrix and then all excitation cross sections between states in the R-matrix expansion that are energetically allowed (open channels). A simple way of determining the total ionization cross section for close-coupling methods is to sum over all excitation cross sections to open positive energy states.

III. RESULTS

We carried out both time-dependent wave-packet and time-independent T-matrix calculations for the electron-impact ionization of hydrogen in the Temkin-Poet model at an incident energy of 20 eV. Both ejected energy differential and total cross sections are calculated for several wave-packet widths and for several states in the R-matrix expansion related to different box sizes.

A 250×250 point lattice with a uniform mesh spacing of $\Delta r=0.20$ and a box size of $R=50.0$ was first employed for the wave-packet calculations. Probability densities $|P(r_1,r_2,t)|^2$ of the symmetrized wave function are shown in Fig. 1 for times before and after the collision. The initial wave packet at $t=0.0$ is centered at $r_1=0.0$ and $r_2=25.0$, or $r_1=25.0$ and $r_2=0.0$, with a Gaussian width of $w=6.25$. The final wave packet at $t=44.0$ exhibits ridges of high probability density along each r_1 and r_2 axis, corresponding to elastic and inelastic excitation processes, and a broad plane of lower probability density centered along the $r_1=r_2$ line, corresponding to the inelastic ionization process.

A 1600-point lattice with a uniform mesh spacing of $\Delta r=0.025$ and a box size of $R=40.0$ was first employed for the T-matrix calculations. Probability densities $|P_E^+(r_1,r_2)|^2$ of the R-matrix wave function are shown in Fig. 2 for both a one-state and a ten-state expansion. In both cases 51 states were used in the expansion for the continuum electron. For clarity, Fig. 2 exhibits the probability density only out to $r=20.0$. The spacing of the nodes for both wave functions along each r_1 and r_2 axis is given by $\pi/k=2.6$ for an incident energy of 20 eV. The probability density for the one-state R-matrix wave function is found to be identical to the density calculated using the Hartree-Fock distorted wave function of Eq. (9), while the ten-state R-matrix wave function density shows an extended structure for small r due to the inclusion of pseudostates in the representation of the bound electron.

Excitation and total ionization cross sections for electron scattering from hydrogen in the Temkin-Poet model at an
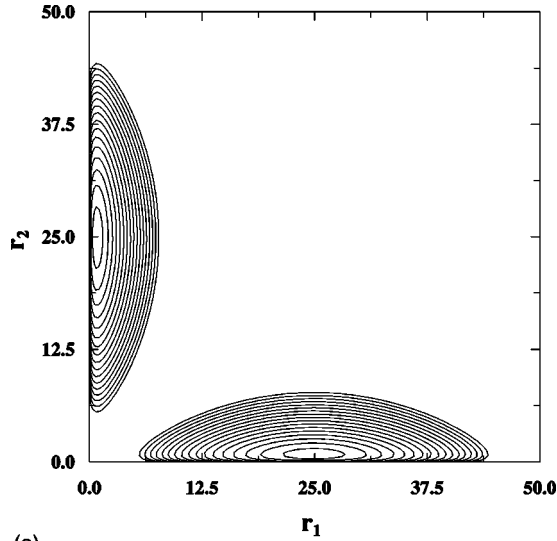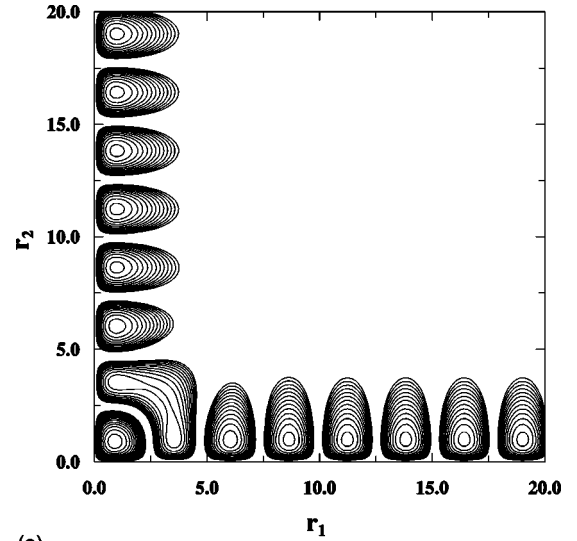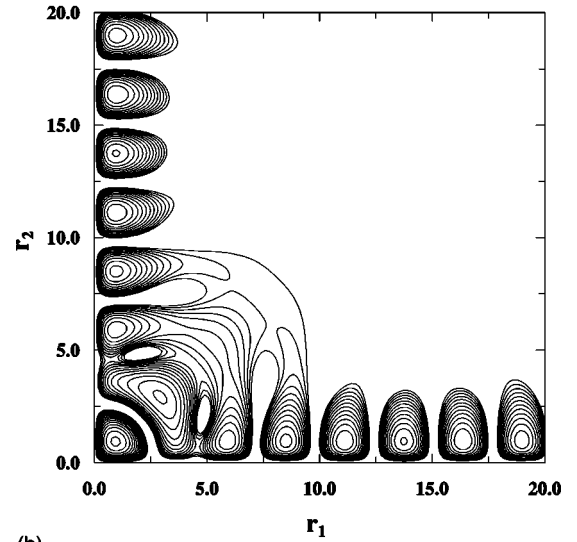
(a)
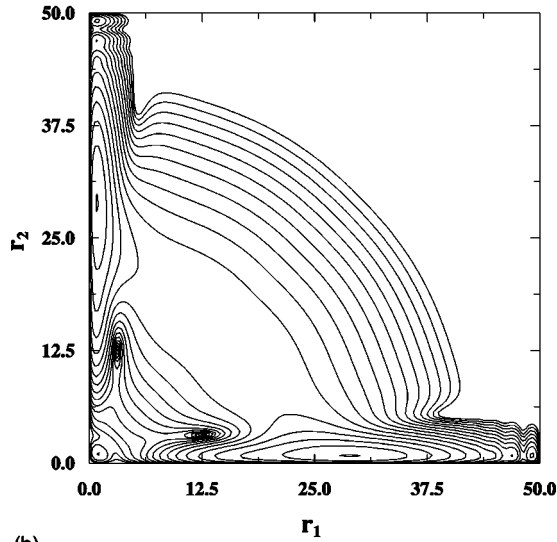
(b)

FIG. 1. Time-dependent scattering solutions for an incident energy of 20 eV. (a) Probability density $|P(r_1,r_2,t=0.0)|^2$ of symmetrized wave packet before collision for a box size of $R=50.0$. (b) Probability density $|P(r_1,r_2,t=44.0)|^2$, of symmetrized wave packet after collision for a box size of $R=50.0$. (r_1 and r_2 are radial distances in atomic units.)

(a)

(b)

FIG. 2. Time-independent scattering solutions for an incident energy of 20 eV. (a) Probability density $|P_E^+(r_1,r_2)|^2$ for a one-state R-matrix calculation with a box size of $R=40.0$. (b) Probability density $|P_E^+(r_1,r_2)|^2$ for a ten-state R-matrix calculation with a box size of $R=40.0$. (r_1 and r_2 are radial distances in atomic units.)

incident energy of 20 eV are presented in Table I for the various time-dependent and time-independent methods. In the upper part of Table I all the time-dependent wave-packet calculations are in excellent agreement with the earlier results of Callaway and Oza [3] obtained by direct numerical integration of the time-independent Schrödinger equation. Keeping a fixed mesh spacing of $\Delta r=0.20$, the wave-packet calculations for $R=100.0$ and 200.0 employed successively larger lattices. The (1000×1000)-point lattice, for example, centered an initial wave packet at $r_1=100.0$ and $r_2=0.0$, or $r_1=0.0$ and $r_2=100.0$, with a Gaussian width of $w=25.0$. In the lower part of Table I the time-independent T-matrix calculations are shown to converge nicely to the time-dependent wave-packet results as one increases the number of states in the R-matrix wave function. Keeping a fixed mesh of Δr

$=0.025$, the T-matrix calculations for $R=60.0$, 80.0, and 100.0 employed successively larger lattices. For an incident energy of 20 eV, the $R=40.0$ lattice of 1600 points supported ten open channels (five bound and five continuum states), while the $R=100.0$ lattice of 4000 points supported 24 open channels (eight bound and 16 continuum states). For the $R=100.0$ lattice, 101 states were used in the expansion for the continuum electron.

As they should be, the distorted-wave and one-state R-matrix results are in excellent agreement for the total ionization cross section. The $1s\rightarrow2s$ excitation cross section drops by 45% from the two-state R-matrix calculation to the larger (10–24)-state R-matrix calculations, while the $1s\rightarrow3s$ excitation cross section drops by almost 50%. This

TABLE I. Excitation and total ionization cross sections (in Mb) at an incident energy of 20 eV. DW, distorted-wave method; RM*n*(R=num), *n*-state R matrix with a box size of R; TDSE(R=num), time-dependent Schrödinger equation method with a box size of R; TISE, time-independent Schrödinger equation method [3]. (1.0 Mb = 1.0×10^{-18} cm^2.)

Method	Excitation $1s \rightarrow 2s$	Excitation $1s \rightarrow 3s$	Ionization	
TDSE(R=50)	2.41	0.59	1.27	
TDSE(R=100)	2.49	0.64	1.29	
TDSE(R=200)	2.50	0.64	1.28	
TISE	2.46	0.62	1.36	
Method	Excitation $1s \rightarrow 2s$	Excitation $1s \rightarrow 3s$	Ionization continuum sum	Ionization T matrix
DW				3.08
RM1(R=40)				3.06
RM2(R=40)	4.63			2.98
RM3(R=40)	4.39	1.29		2.84
RM4(R=40)	4.16	1.30		2.73
RM5(R=40)	3.77	1.21		2.48
RM6(R=40)	3.13	1.02	0.96	2.45
RM8(R=40)	2.44	0.66	1.42	1.44
RM10(R=40)	2.54	0.68	1.21	1.29
RM15(R=60)	2.46	0.62	1.38	1.34
RM19(R=80)	2.52	0.66	1.36	1.32
RM24(R=100)	2.50	0.65	1.30	1.26

reduction is due to coupling to the higher-energy bound and continuum pseudostates. Only for the six-state R-matrix calculation (five bound and one continuum) is there any appreciable difference between the total ionization cross section calculated using the T-matrix method and the much simpler sum over open positive energy excitations. Although not shown in Table I, we extended the R=40.0 lattice calculations for the R-matrix wave function to include 14 states (ten open and four closed) with very little change in the excitation and total ionization cross sections. We also carried out R=40.0 lattice calculations at a fixed mesh of $\Delta r = 0.0125$, and thus 3200 points, with again very little change in the inelastic cross sections.

Ejected energy differential ionization cross sections for electron scattering from hydrogen in the Temkin-Poet model at an incident energy of 20 eV are presented in Fig. 3. The upper solid curve is a T-matrix calculation using a Hartree-Fock distorted wave. The lower solid curve in Fig. 3 is a time-dependent wave-packet calculation for R=50.0. The dashed curves are various T-matrix calculations with one state, three states, five states, and ten states in the R-matrix wave-function expansion for a box size of R=40.0. Unphysical oscillations appear in the differential cross sections for all R-matrix results involving more than three states in the expansion. However, the oscillations produced in the differential cross section by the ten state R-matrix wavefunction are small, symmetric about $E/2$, and bracket the smooth shape of the time-dependent wave-packet results. A 14-state R-matrix expansion with R=40.0, including ten open and four closed channels, yields a cross section quite similar to

that shown for the ten state calculation.

Further ejected energy differential ionization cross sections are presented in Fig. 4 for an incident energy of 20 eV. The upper solid curve is again a T-matrix calculation using a Hartree-Fock distorted wave. The lower solid curve in Fig. 4 is a time-dependent wave-packet calculation for R=200.0. In agreement with other recent work [12–14], the larger-lattice time-dependent wave-packet results begin to show a V-shape dependence centered at $E/2$. The upper dashed curve is a T-matrix calculation with one state in the R-matrix
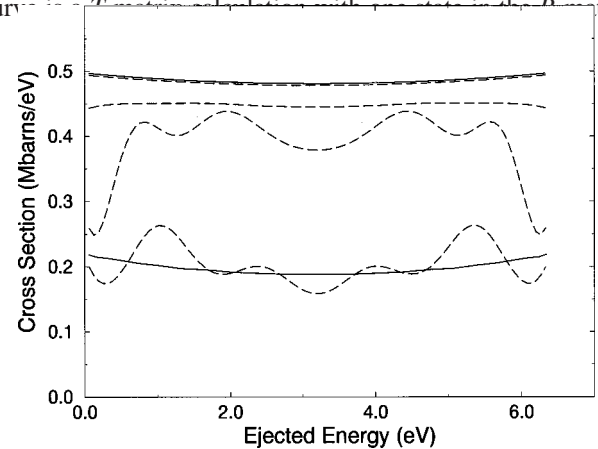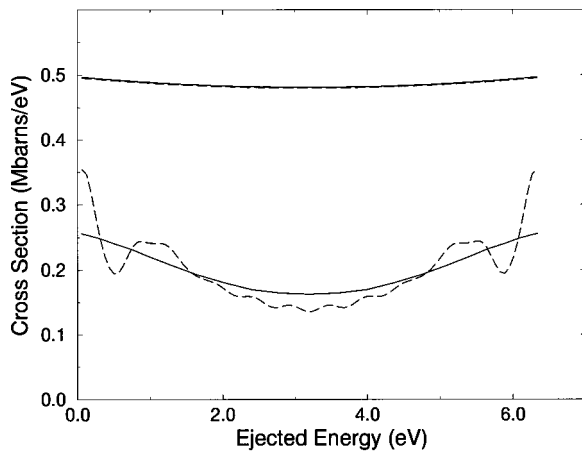

FIG. 3. Ejected energy differential cross sections for an incident energy of 20 eV. Solid curves: upper, distorted-wave method; lower, time-dependent wave-packet method with a box size of R=50.0. Dashed curves from top to bottom: T-matrix method with one state, three states, five states, and ten states in the R-matrix expansion with a box size of R=40.0.

FIG. 4. Ejected energy differential cross sections for an incident energy of 20 eV. Solid curves: upper, distorted-wave method; lower, time-dependent wave-packet method with a box size of $R = 200.0$. Dashed curves: upper, T-matrix method with one state; lower, T-matrix method with 24 states in the R-matrix expansion with a box size of $R = 100.0$.

wave-function expansion and the lower dashed curve is a T-matrix calculation with 24 states, both for a box size of $R = 100.0$. The 24-state R-matrix calculation begins to show a V-shape dependence with quite small oscillations near $E/2$, and again tracks the time-dependent wave-packet results quite well. We expect that the wave-packet and T-matrix methods will yield a more pronounced V-shaped differential cross section for $R \geqslant 500.0$ box sizes.

IV. SUMMARY

In this paper we have shown that an eigenchannel R-matrix expansion of the T matrix may be formulated and used to calculate accurate total integrated and ejected energy differential cross sections for the electron-impact ionization of hydrogen in the Temkin-Poet model. The formulation itself avoids the step-function problem in that it produces a

symmetric ejected energy differential cross section about $E/2$. The largest R-matrix expansions yield differential cross sections that track well the results given by a time-dependent wave-packet method.

Unphysical oscillations appear in the differential ionization cross sections for all T-matrix results involving more than three states in the R-matrix expansion. For the largest R-matrix expansions the oscillations are found to be small and symmetric about $E/2$, while tracking the smooth time-dependent wave-packet results. At the relatively low incident energy of 20 eV, both the time-dependent wave-packet and the time-independent T-matrix calculations for the differential ionization cross section are found to be somewhat sensitive to the overall box size. For larger box sizes, both methods produce differential ionization cross sections that begin to show a V-shaped dependence around $E/2$ that is characteristic of recent results obtained using the hyperspherical close-coupling method [12] and the exterior complex scaling method [13], and by direct numerical integration of the time-dependent Schrödinger equation [14].

In the future we hope to formulate and impliment a Wigner-Eisenbud R-matrix expansion of the T matrix. Instead of pseudostates in the bound electron expansion of the wave function that vanish only at the boundary, one could use pseudostates that exponentially decay at the boundary, like Sturmian functions [9]. We again expect to find small oscillations in the total and differential ionization cross sections that may be easily averaged to yield smooth and accurate predictions for a variety of atomic systems.

[1] A. Temkin, Phys. Rev. **126**, 130 (1962).
[2] R. Poet, J. Phys. B **11**, 3081 (1978).
[3] J. Callaway and D. H. Oza, Phys. Rev. A **29**, 2416 (1984).
[4] M. LeDourneuf, J. M. Launay, and P. G. Burke, J. Phys. B **23**, L559 (1990).
[5] I. Bray and A. T. Stelbovics, Phys. Rev. Lett. **69**, 53 (1992).
[6] S. Watanabe, Y. Hosoda, and D. Kato, J. Phys. B **26**, L495 (1993).
[7] K. W. Meyer, C. H. Greene, and I. Bray, Phys. Rev. A **52**, 1334 (1995).
[8] W. Ihra, M. Draeger, G. Handke, and H. Friedrich, Phys. Rev. A **52**, 3752 (1995).
[9] K. Bartschat and I. Bray, Phys. Rev. A **54**, R1002 (1996).
[10] C. W. McCurdy, T. N. Rescigno, and D. Byrum, Phys. Rev. A **56**, 1958 (1997).
[11] I. Bray, Phys. Rev. Lett. **78**, 4721 (1997).
[12] N. Miyashita, D. Kato, and S. Watanabe, Phys. Rev. A **59**, 4385 (1999).
[13] M. Baertschy, T. N. Rescigno, W. A. Isaacs, and C. W. McCurdy, Phys. Rev. A **60**, R13 (1999).
[14] S. Jones and A. T. Stelbovics, Phys. Rev. Lett. **84**, 1878 (2000).
[15] I. E. McCarthy and Z. Xixiang, in *Computational Atomic Physics*, edited by K. Bartschat (Springer, New York, 1996), p. 87.
[16] P. G. Burke and K. T. Taylor, J. Phys. B **8**, 2620 (1975).
[17] F. Robicheaux, M. S. Pindzola, and D. R. Plante, Phys. Rev. A **55**, 3573 (1997).
[18] M. S. Pindzola and F. Robicheaux, Phys. Rev. A **55**, 4617 (1997).
[19] M. S. Pindzola and F. Robicheaux. Phys. Rev. A **61**, 052707 (2000).
[20] C. Bottcher, J. Phys. B **14**, L349 (1981).